13th World Conference on Earthquake Engineering
Vancouver, B.C., Canada
August 1-6, 2004
Paper No. 443

SEISMIC PERFORMANCE OF HIGH-RISE RC FRAME STRUCTURE USING ULTRA HIGH STRENGTH CONCRETE

Akiko SANADA[1] and Makoto MARUTA[2]

SUMMARY

In Japan, high-rise RC frame technology has been developing since the first high-rise RC frame was constructed in 1974. Recently, high-rise RC frame structures of over 50 stories have been planned. Columns in the lower stories of high-rise RC frames are subjected to high long-term compressive axial forces, and the exterior columns are also subjected to high variable axial forces due to overturning moments under large earthquakes. Therefore, high axial strength columns using high strength materials have been required to resist earthquake forces. However, the structural performance of high strength columns under high axial force is not clear. Therefore, three kinds of experimental studies (column and beam-column subassemblages) were carried out to investigate the seismic performance of high strength column and beam-column subassemblages. A total of 30 specimens were tested. These specimens were constructed with high strength concrete (Fc=100MPa ～170MPa). The cracking behavior, ultimate strength and hysteresis characteristics were obtained from the test results. The cracking strength and ultimate strength can be evaluated by the existing method for normal RC members and the newly proposed method described in this paper.

Sufficient reinforcement by high strength hoops improves column's deformation capacity. Through this study, the seismic performance of high strength RC frames was examined, making it possible to design RC structure of over 50 stories in a seismic country.

INTRODUCTION

Columns and beam-column subassemblages (joints, hereafter) in the lower story of a high-rise RC building are subjected to high long-term axial load. In particular, the exterior columns and joints are also subjected to high variable axial forces due to overturning moment under a large earthquake. High strength columns and joints using high strength materials are required to resist these earthquake forces. However, there have been few studies on the structural performance of high strength columns and joints under high axial forces. Therefore, three kinds of experimental studies (two on columns[1)] and one on joints) were carried out to investigate the seismic performance of high strength columns and joints. This paper outlines these three kinds of experimental studies and evaluates the cracking strength, ultimate strength and

[1]Research Engineer, Kajima Technical Research Institute, Tokyo, JAPAN, Email:akikokmr@kajima.com
[2]Supervisory Research Engineer, Kajima Technical Research Institute, Email: maruta@kajima.com

ductility obtained from these tests. As a result, adequate formulas to estimate flexural and shear strength were proposed for columns and joints made high strength materials.

STRUCTURAL TEST OF HIGH STRENGTH COLUMN

Outline of Test

Table 1 lists seven specimens, their material properties and experimental results. The specimens were about 1/3 scale. Three kinds were used: exterior columns in the lowest story (LE series), exterior columns in the lower story (SE series) and interior columns in the lowest story (LI series). Typical details of the exterior columns in the lowest story (LE7) and the section of a column loaded in the 45-degree direction (LE10-45) are shown in Fig.1. The shear span ratios (M/QD) of the lowest story columns (LE & LI series) and the lower story columns (SE series) were 2.5 and 1.5, respectively.

The specimens were made of high strength concrete (Fc=100MPa), high strength longitudinal bars (D19-SD685) and high strength hoops (D6-SD785). Welded closed circular and square hoops were used in all specimens. LE and SE series were tested under varying axial forces and LI series was tested under constant axial force. Fig.3 shows the relationship between the applied bending moment (M) and the axial force (N). First, LE and SE series were subjected to a long-term axial force (0.2cNu: cNu: compressive strength of column). Next, a varying axial force proportional to the bending moment was applied to the specimen. The axial force varied between 0.7cNu on the compressive side and 0.75tNu (tNu: tensile strength of column) on the tensile side.

Table 1 Reference of The Test (Test of HSC Column)

Location	Specimen	M/QD	Axial Force	Pw [1] %	Compressive Strength Of Concrete (N/mm^2)			Test Results (kN·m)		Calculated Strength (kN·m)			
					σ_B [2]	$_C\sigma_{SA}$ [3]	$_C\sigma_{MA}$ [4]	$_EM_{BC}$ [5]	M_{BMAX} [6]	$_CM_{BC}$ [7]	M_{BACI} [8]	$_CM_{BSA}$ [9]	$_CM_{BMA}$ [10]
Exterior Column	LE7	2.5	0.75tNu ~ 0.7cNu	0.7	112	120 [1.07]	124 [1.10]	377	433	395 (0.95)	286 (1.51)	399 (1.09)	408 (1.06)
	LE10			1.0	114	126 [1.11]	129 [1.13]	391	458	395 (0.99)	292 (1.57)	417 (1.10)	427 (1.07)
	LE10-45			1.0	113	125 [1.07]	128 [1.10]	413	461	395 (1.04)	243 (1.90)	392 (1.18)	407 (1.13)
	SE7	1.5		0.7	116	124 [1.07]	128 [1.10]	349	395	396 (0.88)	298 (1.33)	414 (0.95)	423 (0.93)
	SE10			1.0	119	131 [1.10]	135 [1.13]	419	562	396 (1.06)	308 (1.82)	436 (1.29)	447 (1.26)
Interior Column	LI9	2.5	0.3cNu	0.9	106	116 [1.10]	120 [1.13]	213	541	178 (1.20)	380 (1.41)	470 (1.15)	473 (1.14)
	LI12		0.6cNu	1.2	115	129 [1.12]	132 [1.14]	374	455	323 (1.16)	348 (1.55)	453 (1.00)	421 (1.08)

[1]Hoop Ratio, [2] Compressive Strength of Concrete by Cylinder Test, [3] Compressive Strength of Confined Concrete by Sakino Model[4], [4] Compressive Strength of Confined Concrete by Maruta Model[5], [5] Flexural Cracking Strength [6]Maximum Strength Considering P-Δ Effect [7] The Flexural Cracking Strength by The AIJ[3], [8]The Flexural Strength by ACI Stress Block Method[2], [9], [10] The Flexural Strength Considering Confined Concrete by Sakino and Maruta, [ ] : $_C\sigma/\sigma_B$, ( ) : $_EM_{BC}/M_{BC}$, M_{BMAX}/M_B, The Yielding Strength of Reinforcement, Hoop: 1053 MPa, Longitudinal Bar: 722MPa

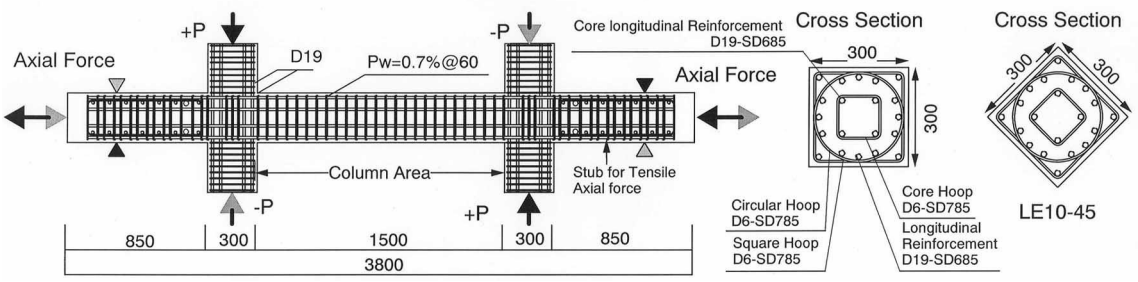

Fig.1 Outline of Specimen (Test of HSC Column)

Experimental Results

Hysteretic responses

Fig.2 shows the load-deflection curves for 6 specimens. P-Δ effects and flexural strength calculated by the ACI method[2] are also plotted on the graphs. After flexural compressive yielding of the longitudinal bars, axial collapse was observed at the final stage. None of the columns showed a remarkable failure mode such as shear failure or flexural failure. When the column was sufficiently reinforced with high strength hoops and subjected to low axial force, it showed good ductility. The column subjected to 45-degree loading (LE10-45) showed almost the same hysteresis characteristics as LE10. A column with a lot of high strength hoops and tested under high compressive axial force (LI12) shows good ductility up to rotation angle of 2%.

Ultimate Rotation Angle

When the horizontal load considering P-Δ effects declines to 95% of maximum strength, the deformation at its point is defined as the ultimate rotation angle in this paper. Fig.4 shows the relationships between ultimate rotation angle and $P_w\sigma_{wy}$, axial force ratio, respectively. $P_w\sigma_{wy}$ is hoop ratio P_w multiplied by hoop yield strength σ_{wy}. High $P_w\sigma_{wy}$ of the column makes higher ultimate rotation angle. Even when the

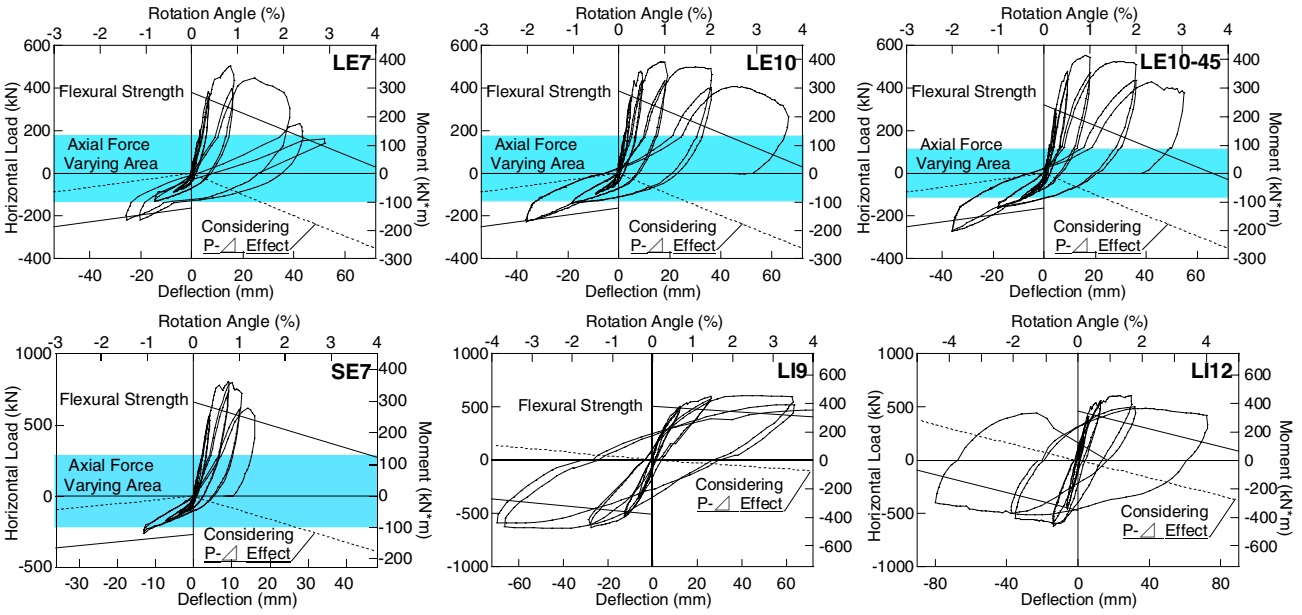

Fig.2 Load-Deflection Curves

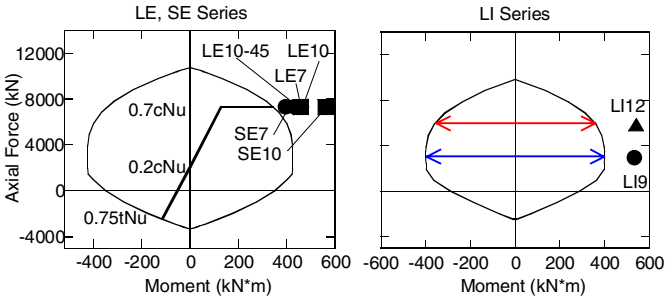

Fig. 3 Bending Moment－Axial Force Relationship

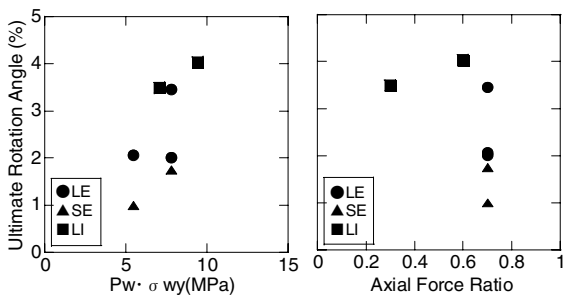

Fig.4 Ultimate Rotation Angle

column was subjected to a high constant compressive axial force of 0.6cNu, the ultimate angle of LI12 with $P_w\sigma_{wy}$=1.2%, was over 4%.

Flexural Strength Considering Confined Concrete

Table 1 compares the test flexural cracking strength (compressive side) with the calculated strengths by the AIJ Standard as shown in Table 1. The calculated flexural cracking strengths showed good correspondence with the test results.

The flexural cracking strength of columns proposed in AIJ[3] are given in Eq.1.

$$_C M_{BC} = 0.56\sqrt{\sigma_B} \cdot Ze + \frac{N \cdot D}{6} \qquad \text{(kN*m)} \qquad (1)$$

σ_B : compressive strength of concrete
Ze : section modulus considering longitudinal bars
N : axial force
D : depth of section

Fig.3 shows the M-N interaction curves and the maximum moment obtained from the test results. The M-N interaction curves were calculated by the ACI stress block method[6]. The flexural strength calculated by ACI stress block method was quite lower than the test results. This method assumes that concrete stress distribution is expressed as an equivalent rectangular compression zone, and the strain at the edges of the cross section is 0.003. However, the maximum strength from the tests was much higher than that from the calculations. This is because of the assumed of 0.003 strain and the effect of confined concrete were not considered.

The Sakino model[4] and the Maruta-Suzuki model[5] were used to evaluate the compressive strength of confined core concrete. The compressive strengths of confined concrete proposed by the Sakino and Maruta-Suzuki were 1.07~1.14 times higher than the uniaxial compressive strength of a concrete cylinder[1]. A fiber flexural analysis was conducted using these compressive strengths. The ultimate flexural strength obtained from this analysis showed good correspondence with the maximum strength.

ACI stress block method was effective for concrete with compressive strength lower than 57MPa. The stress block distribution, strain at the edges of the cross section and stress-strain relationships of high strength concrete need to be investigated to extend the ACI stress block method to over 100MPa concrete.

SHEAR TEST OF HIGH STRENGTH COLUMN

Outline of Test

Table 2 lists 14 specimens, their material properties and their test results. The scale of the specimens was 1/4.5. Typical details of the specimens are shown in Fig.5. The shear span ratio (M/QD) was fixed as 1.0 to ensure that it failed in shear. These specimens used high strength concrete of Fc=120MPa and high strength longitudinal bars D13-SD785. The parameters of this test were the hoop configuration (square hoop-sub tie, square hoop-circular spiral hoop combination), hoop ratio P_w (P_w=0.3, 0.6, 1.2, 1.8%), axial force ratio (N/cNu=0.15, 0.3, 0.6) and the combination of strength and hoop diameter (D6-SD785, ω5.1-SBPR1275, ω: strand & diameter, SBPR: specified yield strength (MPa)). To determine the columns' shear capacities under high axial force, 8 specimens were subjected to high axial force of 0.6cNu. The real compressive strength of the concrete became 121~130MPa at the test. According to the loading rule, a constant axial force was applied first, and then reversed cyclic load was applied.

Experimental Results

Table 2 shows lists of the test results. All the data in Table 2 are considering P-Δ effect. Except for H-1.8-0.6 specimen, the longitudinal bars did not yield up to the maximum strength. After yielding of the hoops, immediate axial collapse under high compressive axial force was observed in several specimens. All the specimens failed in shear at the final stage. When the hoop configurations and hoop ratios were all the same, the maximum strengths were almost the same and there was no influence of the axial force. The maximum strength of the H series specimens confined by square and tie hoops was 15~20% larger than that of HS and U series specimens confined by square and circular spiral hoops.

Fig.6 presents the envelope curve obtained from the H series test results. Fig. 6(a) and Fig.6 (b) show the influence of hoop ratio P_w on the hysteresis curve under axial forces of 0.3cNu and 0.6cNu, respectively. Comparing their curves, the specimen adequately reinforced by hoops or loaded under low axial force had high ductility. Sufficient hoop reinforcement made high maximum strength at the test. Fig.6 (c) shows that the maximum shear strength was not influenced by axial force.

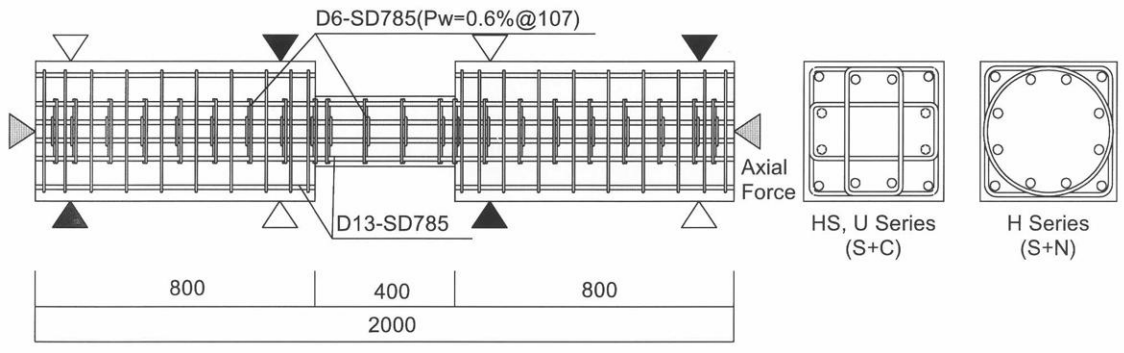

Fig.5 Outline of Specimen (Shear Test of HSC Column)

Table 2 Reference of The Test (Shear Test of HSC Column)

Specimen	Hoop Configuration (Series)	Axial Force Ratio	Hoop			σ_B (MPa)	Test Result (kN)		Calculated Value (kN)		
			Pw (%)	σwy (MPa)	Pw・σwy[1] (MPa)		${}_EQ_{SCR}$[2]	Q_{SMAX}[3]	${}_CQ_{SC}$[4]	$Q_{S\text{-}AIJ}$[5] Rp=0	$Q_{S\text{-}NewRC}$[6]
H-0.6-0.15	S+N (H)	0.15	0.6	D6 785	4.7	128	270	522	244 (1.08)[7]	439 (1.19)	455 (1.15)
H-0.6-0.3		0.3				125	367	516	330 (1.07)	439 (1.18)	475 (1.09)
H-0.6-0.6		0.6				120	466	523	452 (0.98)	439 (1.19)	641 (0.82)
HS-0.6-0.3	S+C (HS)	0.3				128	400	494	332 (1.17)	439 (1.13)	475 (1.04)
HS-0.6-0.6		0.6				128	445	508	460 (0.94)	439 (1.16)	641 (0.79)
HS-1.2-0.6			1.2		9.4	129	533	588	461 (1.13)	604 (0.97)	802 (0.73)
H-0.3-0.6	S+N (H)	0.6	0.3		2.4	128	431	485	460 (0.91)	321 (1.51)	561 (0.86)
H-1.2-0.6			1.2		9.4	121	555	681	453 (1.17)	604 (1.13)	802 (0.85)
H-1.8-0.6			1.8		14.1	130	588	778	462 (1.24)	664 (1.17)	962 (0.81)
H-0.3-0.3		0.3	0.3		2.4	130	394	524	334 (1.16)	321 (1.63)	409 (1.28)
H-1.2-0.3			1.2		9.4	121	354	689	327 (1.04)	604 (1.14)	607 (1.13)
H-1.8-0.3			1.8		14.1	121	439	798	327 (1.29)	664 (1.20)	739 (1.08)
U-0.4-0.6	S+C (U)	0.6	0.37	φ 5.1 1275	4.7	130	478	508	462 (1.01)	408 (1.25)	605 (0.84)
U-0.7-0.6			0.74		9.4	129	506	561	461 (1.07)	578 (0.97)	728 (0.77)

S: Square Hoop, N: Tie Hoop, C: Circle Spiral Hoop, Yielding Strength of Reinforcement D6 : 1053MPa*, φ 5.1 : 1450MPa D13 : 1030MPa*
* : 0.2% Offset Value, [1] Hoop Quantity [2] Shear Cracking Strength [3] Maximum Strength [4] Shear Cracking Strength by Eq.2, [5] Shear Strength by AIJ[6] [6] Shear Strength by NewRC[7] [7] Test Result/ Calculated Value, Specimen : H- 0.6 - 0.6 (Hoop Configuration)-(Pw(%))-(Axia Force Ratio)

Shear Strength

Table 2 lists the shear cracking strength [2] and the maximum strength [3] obtained from the test results, and those obtained from calculations. The calculation methods used the principal stress formula for shear cracking, and the estimation method by AIJ[6] [5] and NewRC[7] [6] for the ultimate shear strength. In AIJ formula, an effective coefficient (ν_0) of effective concrete strength for shear was defined by the CEB expression given in Eq.8.

The observed and calculated shear cracking strength showed good correspondence as shown in Table 2. Fig.7 compares the observed maximum strengths with the calculated ones by AIJ and NewRC formulas, respectively. Except for the specimen with P_w=0.3%, the shear strength calculated by AIJ formula for an unyielding member was approximately the same as the test result. The calculated shear strength by NewRC showed good agreement with the result of the test with axial forces from 0.15cNu to 0.3cNu. However, the calculated shear strength by NewRC is higher than the test result with high axial force of 0.6cNu.

The shear cracking strength of a column ${}_cQ_{SC}$ was calculated by the principal stress method given in Eq.2.

$$ {}_cQ_{SC} = b \cdot D \cdot \sqrt{\sigma_T^2 + \sigma_T \cdot \sigma_0} / \kappa \quad \text{(kN)} \tag{2} $$

b : width of section
D : depth of section
σ_T : tensile strength of concrete=$0.313\sqrt{\sigma_B}$ (MPa)
σ_0 : axial compressive stress
κ : shape factor of section

The shear strength of a ductile column $Q_{S\text{-}AIJ}$ adopted in AIJ Guideline[6] are given in Eq.3, where the value of $P_w\sigma_{wy}$ takes $\nu_0\sigma_B/2$ when $P_w\sigma_{wy}$ exceeds $\nu_0\sigma_B/2$.

$$ Q_{S-AIJ} = b\, j_t P_w \sigma_{wy} \cot\phi + \tan\theta(1-\beta) bD\nu\sigma_B / 2 \quad \text{(kN)} \tag{3} $$

$$ \tan\theta = \left\{\sqrt{(L/D)^2 + 1}\right) - L/D\right\} \tag{4} $$

$$ \beta = \left\{\left(1 + \cot^2\phi\right) P_w \sigma_{wy}\right\} / (\nu\sigma_B) \tag{5} $$

$$ \cot\phi = \min(j_t / [D\tan\theta], \sqrt{\nu\sigma_B / P_w \cdot \sigma_{wy} - 1.0}, 2.0 - 50R_P) \tag{6} $$

$$ \nu = (1.0 - 15R_P)\nu_0 \tag{7} $$

$$ \nu_0 = 1.70\sigma_B^{-0.333} \quad \text{(MPa)} \tag{8} $$

The shear strength of ductile columns $Q_{S\text{-}NewRC}$ proposed by the NewRC Project[7] is given in Eq.9, where the value of $P_w\sigma_{wy}$ takes $\nu_0\sigma_B/2$ when $P_w\sigma_{wy}$ exceeds $\nu_0\sigma_B/2$.

$$ Q_{S-NewRC} = bj_t P_w \cot\phi + \alpha(1-\beta) bD\nu\sigma_B \tag{9} $$

$$ \sigma_{wy} \le 125\sqrt{\nu_0\sigma_B} \tag{10} $$

$$ \alpha = \left\{\sqrt{1 + (L/D)^2} - L/D\right\} / 2 \tag{11} $$

$$ \beta = (1 + \cot^2\phi) P_w \sigma_{wy} / (\nu\sigma_B) \tag{12} $$

$$ \nu = (1.0 - 15R_p) \cdot \nu_0 \tag{13} $$

$$ \nu_0 = 1.70(1 + 2n)\sigma_B^{-0.333} \quad \text{(MPa)} \tag{14} $$

$$\cot\phi = \min(2.0 - 3n - 50R_p,\ j_t / (2\alpha D),\ \sqrt{\nu\sigma_B / (P_w\sigma_{WY}) - 1.0}) \quad (15)$$

jt : distance between top and bottom longitudinal bars
P_w : hoop ratio
σ_{wy} : hoop yield strength
L : clear span length of column
$\nu_0\sigma_B$: effective strength of concrete
ϕ : angle of strut in truss mechanism
R_P : plastic drift angle in the yield hinge region
n : axial load ratio given by $n=N/(bD\sigma_B)$

Ultimate Rotation Angle

Fig.8 illustrates the ultimate rotation angle-$P_w\ \sigma_{wy}$ relationship. The ultimate rotation angle is usually used for members that failed in flexure. Just for this reference, this angle is used for the shear ductility index.

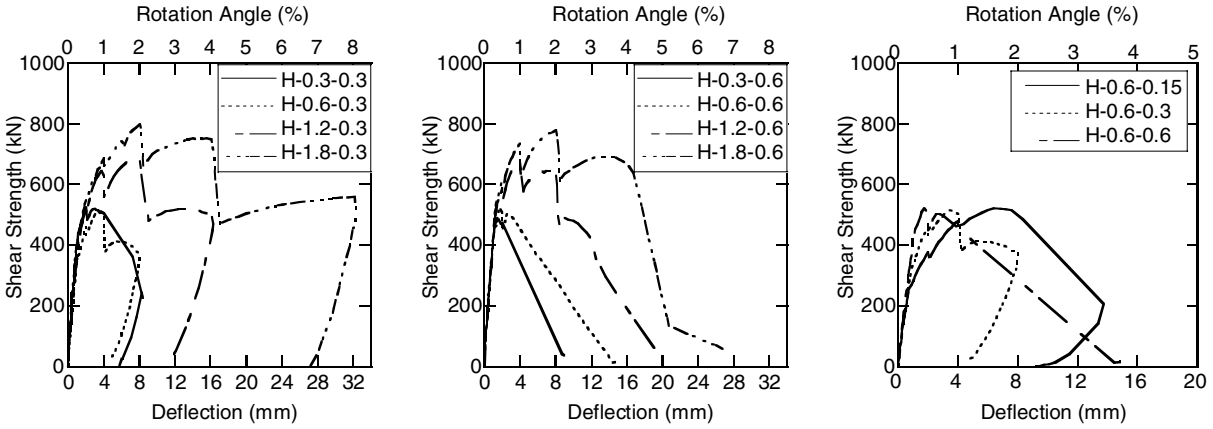

(a) N=0.3cNu **(b) N=0.6cNu** **(c) Pw=0.6%**

Fig.6 Envelope Curve of Load-Deflection Relationship

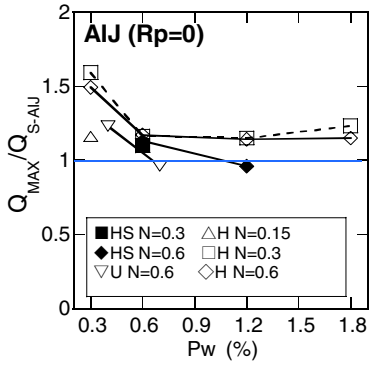

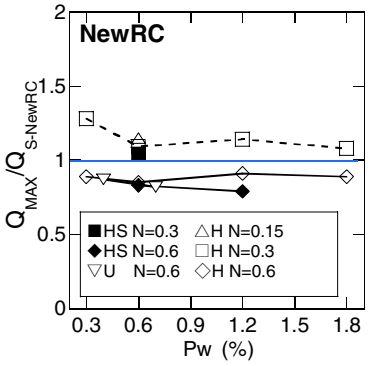

Fig.7 Comparison of Observed and Calculated Strength

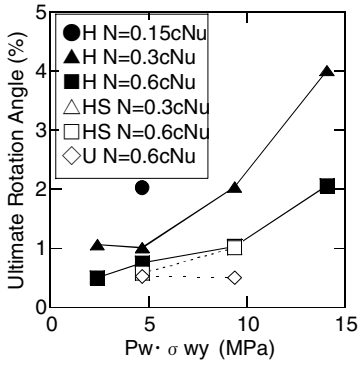

Fig.8 Ultimate Rotation Angle

It is clear from these figures that the ductility of the members that failed in shear is also influenced by axial force and hoop ratio. H-1.8-0.6 specimen, which was subjected to a high axial force 0.6cNu could deform over 2% because of the sufficient reinforcement of Pw=1.8% hoop ratio.

STRUCTURAL TEST OF HIGH STRENGTH BEAM-COLUMN SUBSEMBLAGES

Outline of Test

The specimens consisted of 6 exterior beam-column subassemblages (joints, hereafter) of 1/3 scale and 3 interior joints of 1/2.5 scale. Table 3 lists the test specimens. Typical details of the exterior joint TC-1 and the interior joint CC-1 are shown in Fig.9. The shear span ratios (M/QD) of the columns and the beams were 1.5 and 3.0, respectively.

The parameters of the exterior joint were the axial force (TC series: constant compressive axial force, TV series: variable axial force) and the ratio of beam to joint shear strength. The expected failure mode of each specimen is as follows. TC and TV-1 were expected to suffer joint shear failure before beam flexural yielding (failure mode J), TV-2 was expected to suffer joint shear failure after beam flexural yielding (failure mode BJ), TV-3 was expected to suffer beam flexural yielding (failure mode B), as shown in Table 4. In TC and TV-1, high strength longitudinal bars of D19-SD685 were used for the beams. In TV-2 and TV-3, normal strength longitudinal bars of D19-SD490 and normal strength concrete (Fc=60MPa) were used for the beams. The compressive strength of the concrete was 175~179 MPa at the test. The TV series specimens were subjected to a long-term axial force (0.2cNu) at first, and then subjected to varying axial force proportional to the beam end moment. The axial force was varied in the range from 0.7cNu on the compressive side to 0.75tNu on the tensile side. The column was supported by pins at each end, and vertical reversed cyclic load were applied to the beam end.

The parameters of the interior joints were the concrete strength of joint and the quantity of beam longitudinal bars. CC-1and CC-2 was expected to suffer joint shear failure (failure mode J) and CC-3 was expected to suffer joint shear failure after beam flexural yielding (failure mode BJ). CC-1 specimen used high strength concrete (Fc=130MPa). CC-2 and CC-3 used high strength concrete (Fc=170MPa).

CC-3 used normal strength longitudinal bars of D22-SD490. The compressive strengths of the concrete were 170MPa (CC-1) and about 186~190MPa (CC-2, CC-3) in the test. A constant compression axial force was applied to the column. The column was supported by pins at each end and vertical reversed cyclic load was applied to the beams ends.

Table 3 Lists of the Specimens (Structural Test of HSC Joint)

<table>
<tr><th rowspan="2">Specimen</th><th rowspan="2">Location</th><th colspan="3">Column</th><th colspan="3">Beam</th><th>Joint</th><th rowspan="2">Axial Force</th></tr>
<tr><th>Section</th><th>Longitudinal Bar</th><th>Hoop</th><th>Section</th><th>Longitudinal Bar</th><th>Hoop</th><th>Hoop</th></tr>
<tr><td>TC-1</td><td rowspan="6">Exterior Joint</td><td rowspan="6">300*300</td><td rowspan="3">12-D19 SD685 [1]</td><td rowspan="6">4-Φ6.4@60
SBPR1275 [3]</td><td rowspan="6">220*300</td><td rowspan="3">8-D19 SD685 [1]</td><td rowspan="6">4-Φ6.4@50
SBPR1275 [3]</td><td rowspan="6">4-Φ6.4
SBPR1275 [3]
Pw=0.44%</td><td>0.23cNu</td></tr>
<tr><td>TC-2</td><td>0</td></tr>
<tr><td>TC-3</td><td>0.7tNu</td></tr>
<tr><td>TV-1</td><td rowspan="3">14+4-D19 SD685 [1]</td><td rowspan="2">0.75tNu
~</td></tr>
<tr><td>TV-2</td><td>8-D19 SD490 [2]</td></tr>
<tr><td>TV-3</td><td>6-D19 SD490 [2]</td><td>0.7cNu</td></tr>
<tr><td>CC-1</td><td rowspan="3">Interior Joint</td><td rowspan="3">400*400</td><td rowspan="3">20-D22 SD685 [4]</td><td rowspan="3">4-D8@50
SD785 [6]</td><td rowspan="3">300*400</td><td>10-D22 SD685 [4]</td><td rowspan="3">4-D8@50
SD785 [6]</td><td rowspan="3">2-D8
SD785 [6]
Pw=0.22%</td><td>0.08cNu</td></tr>
<tr><td>CC-2</td><td rowspan="2">0.074cNu</td></tr>
<tr><td>CC-3</td><td>10-D22 SD490 [5]</td></tr>
</table>

Yielding Strength of Reinforcement, TC and TV specimen [1] 784MPa, [2] 539MPa, [3] 1463MPa
CC Specimen [4] 747 MPa, [5] 532 MPa, [6] 1073 MPa

Table 4 Reference of The Test (Structural Test of HSC Joint)

Specimen	σ_B (MPa)		Failure Type		Test Results (kN)		Calculated Value (kN) (Maximum Strength/Calculated Value)			
	Column	Beam	Expected	Test	${}_EQ_{JC}$ [1]	Q_{BMAX} [2]	${}_CQ_{JC}$ [3]	Q_{BFIB} [4]	$Q_{J\text{-}HiRC}$ [5]	$Q_{J\text{-}AIJ}$ [6]
TC-1	179		J	B	220	474	253(0.87)	420(1.13)	256(1.85)	328(1.44)
TC-2	179			BJ	77.1	454	76.6(1.01)	420(1.08)	256(1.77)	328(1.38)
TC-3	175			J	—	383	—	415(0.92)	250(1.52)	318(1.20)
TV-1	175			BJ	325	458	396(0.82)	415(1.10)	250(1.82)	318(1.43)
TV-2	176	56.3	BJ		279	303	399(0.70)	271(1.12)	254(1.19)	324(0.93)
TV-3	176	56.3	B		201	253	399(0.50)	222(1.14)	254(0.99)	324(0.78)
CC-1	170	69.7	J	J	141	584	181(0.78)	654(0.89)	475(1.23)	574(1.02)
CC-2	190				140	587	196(0.71)	654(0.90)	498(1.18)	613(0.96)
CC-3	186		BJ	BJ	120	520	195(0.61)	486(1.07)	496(1.05)	610(0.85)

[1] Shear Cracking Strength of Joint, [2] The Maximum Strength, [3]The Shear Cracking Strength of Joint by Eq.2 (Assuming $\sigma t=0.31\sqrt{\sigma_B}$), [4] The Flexural Strength of Beam by Fiber Bending Analysis, [5] The Shear Strength of Joint by HiRC[8], [5] The Shear Strength of Joint by AIJ[9]

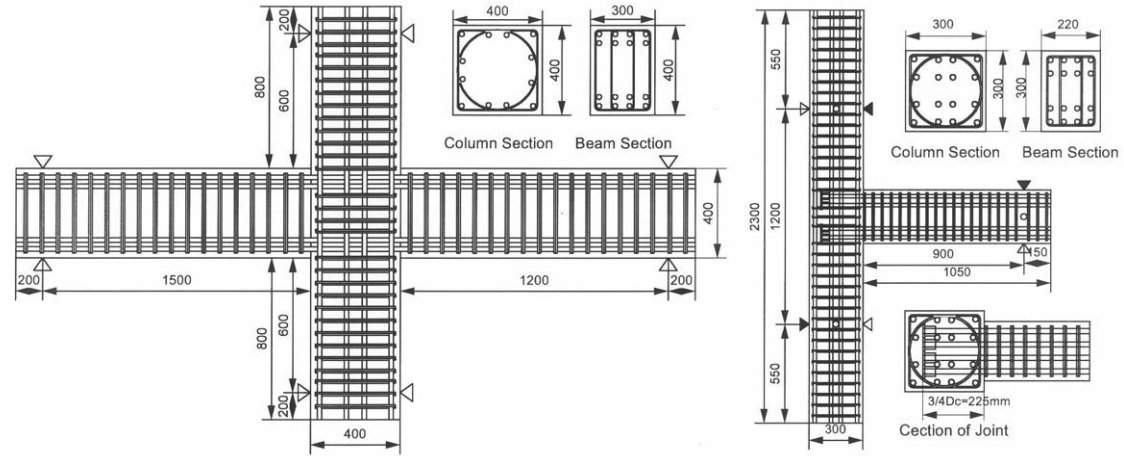

Fig. 9 Outline of Specimen (Structural Test of HSC Joint)

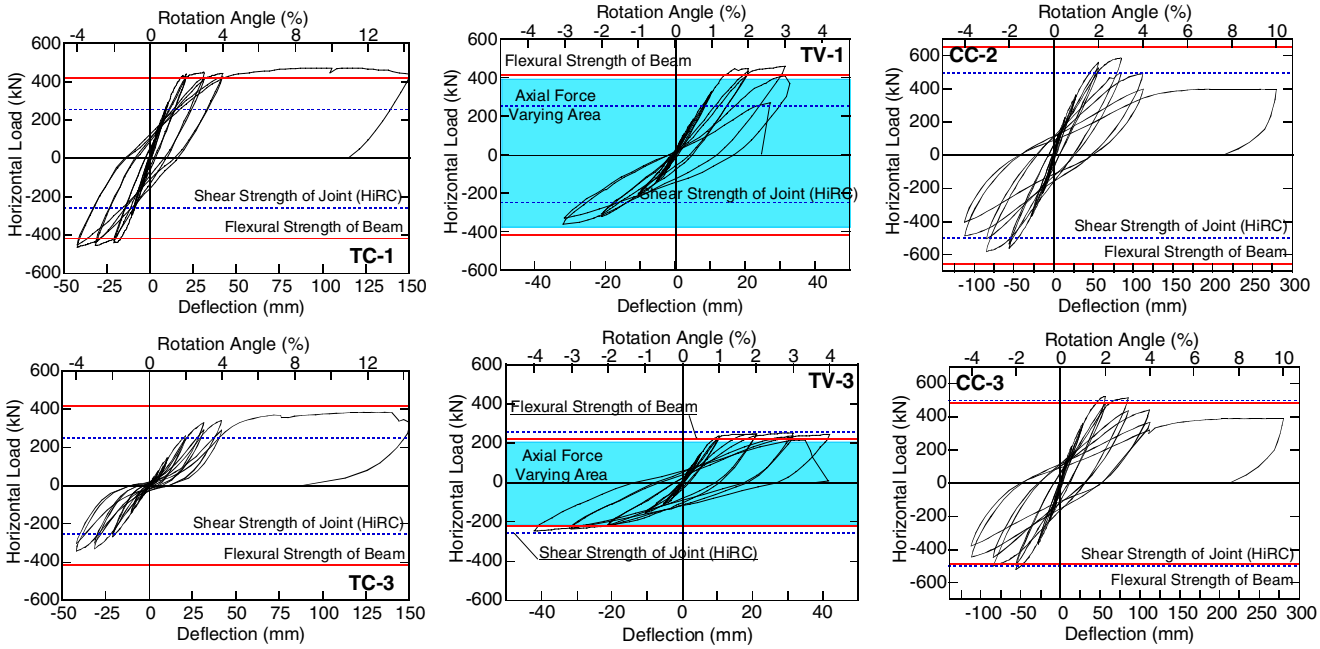

Fig. 10 Load-Deflection Curves

Experimental Results

Table 4 lists the test results and calculated values. Fig.10 shows the load-deflection curves of typical specimens obtained from the test. Except for TC-1 and TC-3, the failure modes of the exterior joint were beam flexural yielding. Joint shear failure was observed at the test of CC-1 and CC-2 specimen, and joint shear failure after beam flexural yielding was observed in CC-3 specimen as shown in Table 4.

TC series, which were exterior joints tested under constant axial force kept their flexural strength up to 14% of interior story drift angle after beam flexural yielding. However, the TV series specimens showed poorer ductile behavior than the TC series, since axial collapse occurred in the joint area on the compressive side. The load deflection curves of TV-1 with TV-3 show that the ductility of the specimen deteriorated with the increase of input shear force into the joint. After reaching maximum strength, a gentle degradation of the horizontal load was observed for the CC series specimens. Although the compressive strengths of the concrete differ, the maximum strength of CC-1 was almost equal to that of CC-2.

Shear Strength of Joint

In Table 4 the shear cracking strength and the maximum strength of the test results are listed and compared with the shear cracking strength of the joint obtained from the principal stress formula assuming κ=1.0, the beam flexural strength calculated by fiber flexural analysis and the joint shear strength calculated by HiRC[8] and AIJ[6]. All the data in Table 4 including the calculated values are presented as the beam-end load for comparison. Fig.11 (a) and Fig.11 (b) presents the relationship between the compressive strength of concrete and the shear strength of interior joint and exterior obtained from this test and the existing data[6], respectively. HiRC formula is also plotted on the Fig.11.

Except for TC-2 specimen, the calculated shear cracking strength of joint exceeded the test results. The maximum strength showed good agreement with the beam flexural strength calculated by fiber-flexural analysis, except for TC-3, CC-1 and CC-2 specimen. The maximum strength of TC-3, CC-1, and CC-3, whose failure modes were failure mode J, can be conservatively estimated by the HiRC formula. In addition, all the data of specimens using various strength of concrete shows good agreement with the HiRC formula as shown in Fig. 11.

The volume of the joint was calculated by multiplying the distance between the center of tension and compression bars of beam j_t, the average of the beam and column width t_p and the horizontal projective length of the anchorage bar D_j, as illustrated in Fig.12.

When the horizontal load at the beam end was Pb, the input shear loads on column Pc and joint Pj shown in Fig.13 are given by Eq.18 and Eq.19, respectively.

(a) Interior Joint

$$M_b = P_b \cdot (L - dc) / 2$$

$$T = T' = Cc + Cs = Cc' + Cs' = M_b / j_b$$

$$P_c = P_b \cdot L / H$$

$$P_j = 2T - P_c = P_b \cdot (L - dc) / j_b - P_b \cdot L / H$$

(b) Exterior Joint

$$M_b = P_b \cdot (L - dc/2) \quad (16)$$

$$T = Cc + Cs = M_b / j_b \quad (17)$$

$$P_c = P_b \cdot L / H \quad (18)$$

$$P_j = T - P_c = P_b \cdot (L - dc/2) / j_b - P_b \cdot L / H \quad (19)$$

The shear strength of joint $V_{J\text{-}HiRC}$ proposed by HiRC[8] is given in Eq.20.

$$V_{J-HiRC} = t_p \cdot D_j \cdot {}_U\tau_P \quad (20)$$

$${}_P\tau_U = p_\beta \cdot p_\gamma \cdot 1.57\sqrt{\sigma_B} \quad \text{(MPa)} \quad (21)$$

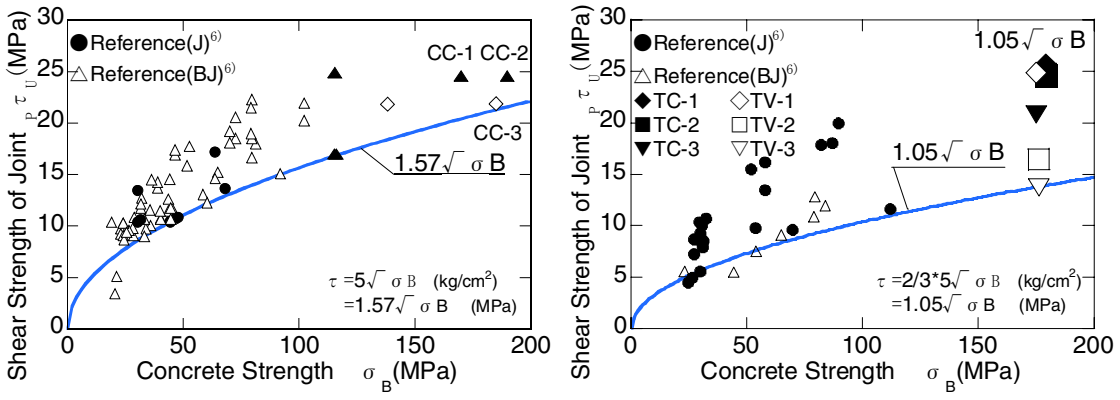

(a) Interior Joint (b) Exterior Joint

Fig. 11 Relationship Between Concrete Strength and Shear Strength of Joint

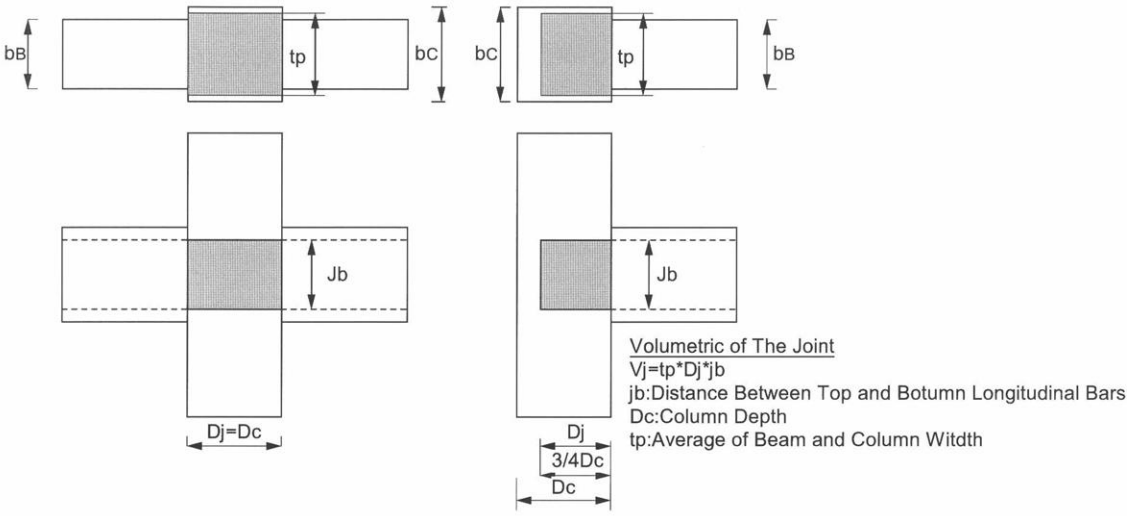

Fig. 12 Estimate Method to Volume of Joint

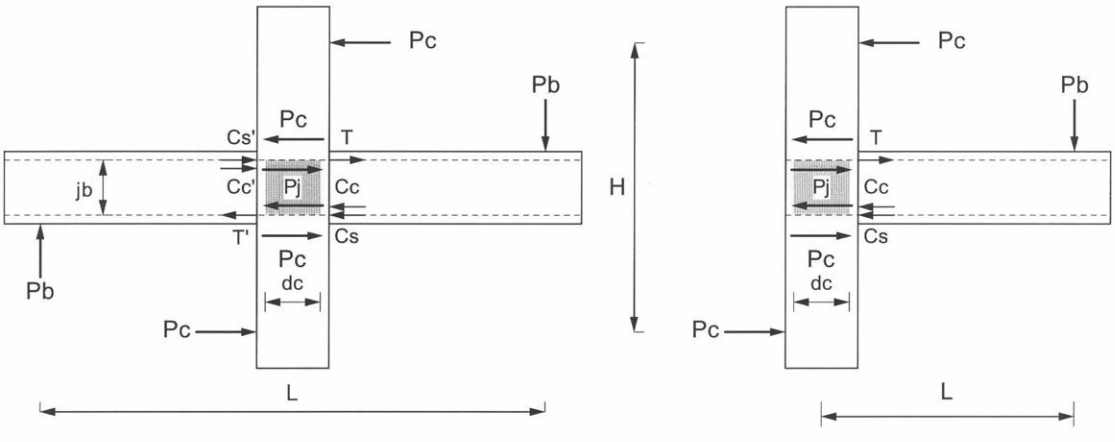

Fig. 13 Balance of Shear Force at Joint

$$t_p = (b_C + b_B)/2 \quad (22)$$

jb : distance between top and bottom longitudinal bars
L : span of beam
tp : average of column and beam widths
D_j : depth of joint
${}_p\tau_u$: shear stress at joint
p_β : shape factor of joint (interior joint p_β=1.0, exterior joint p_β=0.67)
p_γ : confinement factor of joint (without transverse beam p_γ=1.0, with transverse beam p_γ=1.1)

CONCLUSION

Three kinds of experimental studies (two on columns and one on joints) with high strength material such as concrete with compressive strength from 120MPa to 190MPa were carried out to investigate the seismic performance of a high strength RC frame. Following conclusions are obtained.

1) The flexural cracking strength of columns can be calculated by the AIJ formula.
2) The shear cracking strength of columns can be calculated by the principal stress formula.
3) The flexural strength of columns can be calculated by flexural analysis considering confined concrete.
4) The shear strength of columns can be calculated by the AIJ formula, assuming that the rotation drift angle in the yield hinge region is 0.
5) The shear strength of joints can be calculated by the HiRC shear strength of joints.
6) Sufficient reinforcement by hoops is needed for columns to maintain good ductility.
7) Exterior joints under high variable axial force showed poorer ductility than that of interior joints under constant axial force.

REFERENCES

1. Kimura A and Maruta M. "Structural Performance of High Strength RC Columns with 100N/mm^2 Strength Concrete". Proceedings of the first fib congress 2002. Volume 5. PP.715-722. 2002.
2. American Concrete Institute. "Building Code Requirement for Structural Concrete and Commentary". ACI 318-02/318R-02. 2002.
3. Architectural Institute of Japan. "AIJ Standard for Structural Calculation of Reinforced Concrete Structures". 1999.
4. Sun T. P and Sakino K. "Axial Behaviors of Confined High Strength Concrete". Transaction of Japan Concrete Institute. PP.455-462. 1993.
5. Maruta M and Suzuki N. "Axial Compressive Behavior of R/C Columns using Reactanglar and Circular Ties". Proceedings of the JCI. Vol.17. No.2. PP.381-386. 1995(In Japanese).
6. Architectural Institute of Japan. "Design Guidelines for Earthquake Resistant Reinforced Concrete Buildings Based on Ultimate Strength Concept". 1990.
7. Japan Institute of Construction Engineering. "NewRC report". 1993.
8. Maruta M and Bessho S. "Design and Construction of The Highest RC building in Japan". Proceedings of First International Conference of High Strength Concrete. PP.596-609. 1997.